then examined the capacitance of mouse pancreatic beta cells. The technique used is characterised by high time resolution and thus can detect dynamic changes in the cell surface area that reflect exocytosis. Figure 4a shows the capacitance of mouse pancreatic beta cells. Interestingly, adiponectin at a concentration of 10 μg/ml significantly increased the capacitance of mouse pancreatic beta cells to 2.3-fold above baseline (p=0.0091; Fig. 4a), indicating that adiponectin may stimulate insulin granule exocytosis in the absence of any changes in membrane depolarisation, Ca^{2+} currents or $[Ca^{2+}]_c$.

To elucidate the mechanism by which adiponectin increased the exocytosis of insulin-containing granules, we used TIRF microscopy to monitor the real-time docking and fusion process of single insulin granules labelled with a GFP-tagged insulin near the plasma membrane in mouse pancreatic beta cells. Interestingly, adiponectin significantly increased the number of fusion events by newcomers (40.5±4.1 per 200 μm^2 in 0–30 min control beta cells vs 72.3±6.5 per 200 μm^2 in 0–30 min adiponectin-treated beta cells, $p<$0.0005, n=45 for control and n=52 for adiponectin-treated cells; Fig. 4b,c and Electronic supplementary material [ESM], video clips), suggesting that adiponectin may accelerate transport of insulin granules from a cytoplasmic pool to the plasma membrane.

Adiponectin stimulates insulin secretion in vivo To elucidate the physiological roles of adiponectin in insulin secretion in vivo, we studied the effect of adiponectin on insulin secretion in C57BL/6 mice after intravenous transcatheter injection of adiponectin and a low concentration of glucose. We tried to adjust the blood glucose level to approximately 5.6 mmol/l. Figure 5a shows the plasma adiponectin level at 10 and 20 min after the intravenous injection of glucose and saline or adiponectin. The plasma adiponectin levels increased significantly to 1.8 fold of baseline following the injection of adiponectin, while the increased blood glucose levels at 10 and 20 min after the injection were not significantly different between the two groups (Fig. 5b). The blood glucose level and insulin level at the starting point were 3.7±0.4 mmol/l and 36.2±5.0 pmol/l, respectively. No significant differences in the increased plasma insulin levels at 10 min after administration were observed between the adiponectin and the saline groups (Fig. 5c). However, the increase in plasma insulin levels at 20 min after the intravenous injection of glucose was approximately 1.6-fold greater in the adiponectin group (n=19) than in the saline group (n=21; p=0.048; Fig. 5c). We evaluated the changes in ratio of the increment of plasma insulin level to that of blood glucose level. At 20 min after glucose loading the ratio in the adiponectin group was approximately sevenfold higher than that in the saline group (p=0.0088) (Fig. 5d). These results suggest that adiponectin stimulates insulin secretion in vivo.

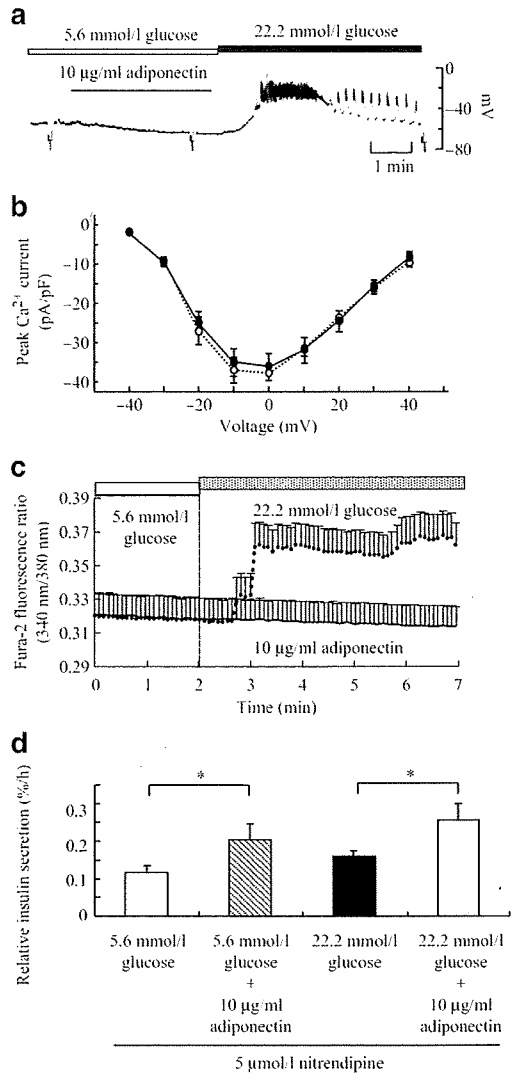

Fig. 2 Adiponectin stimulates insulin secretion without causing membrane depolarisation, closure of K^+_{ATP} – channels or Ca^{2+} entry into the cytosol. **a** Membrane potentials in response to the addition of adiponectin and increasing concentrations of glucose (5.6–22.2 mmol/l) were recorded under the conventional whole-cell mode. Results are representative of three independent experiments. **b** The current–voltage relationships of beta cells treated with (black circles, n=3) or without (white circles, n=3) adiponectin (10 μg/ml). **c** Cytosolic calcium concentrations in response to the addition of adiponectin and increasing concentrations of glucose were measured using fura-2. Mean values are shown (n=5). **d** Islets were incubated in KRB containing the indicated concentrations of glucose and 5 μmol/l nitrendipine with or without 10 μg/ml adiponectin (n=18–23). Values are means±SEM. *p<0.05

Discussion

In this study we have shown that adiponectin stimulates insulin secretion in vitro and in vivo. In addition, our results also indicate that adiponectin stimulates insulin secretion without causing ATP generation, closure of K^+_{ATP}–channels, Ca^{2+} entry into the cytosol or activation of AMPK.

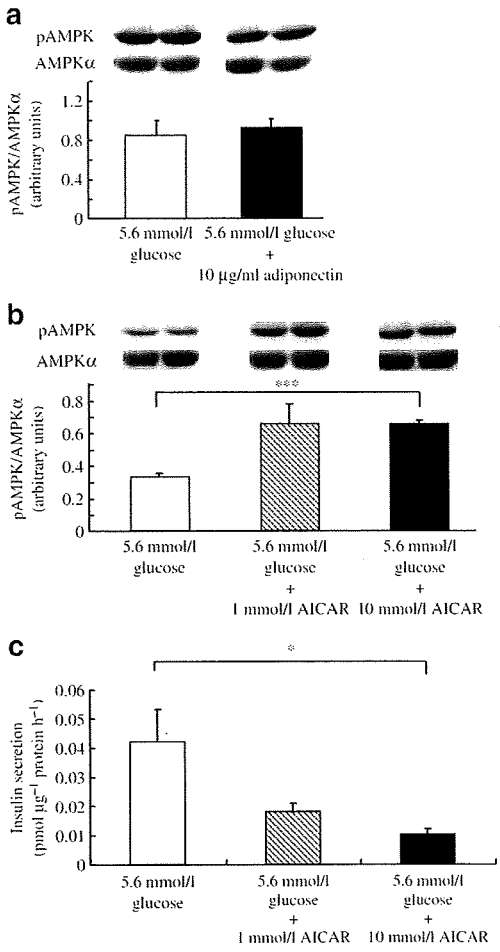

Fig. 3 Adiponectin stimulates insulin secretion without causing activation of AMPK. **a**, **b** Western blots of phosphorylated AMPK and AMPKα in mouse pancreatic islets (n=3, each group). Lysates from 30 islets from each group were subjected to western blot analysis. **c** Isolated islets were incubated with AICAR at 5.6 mmol/l glucose. Values are means±SEM. *p<0.05, ***p<0.001

Adiponectin has previously been reported to increase fatty acid oxidation via activation of AMPK [7, 8], which has been found to increase glucose transport by stimulating the translocation of GLUT4 to the sarcolemma in heart [26] and skeletal muscle [27]. However, adiponectin did not affect the phosphorylation of AMPK in pancreatic islets at 5.6 mmol/l glucose. Since AMPK in pancreatic beta cells is activated by low glucose concentrations [28], adiponectin may be unable to further activate AMPK at this low glucose concentration. By contrast, although the AMPK activator AICAR activated AMPK at this low glucose concentration, AICAR also decreased insulin secretion under these conditions. These results indicate that AMPK is not involved in adiponectin-stimulated insulin secretion at a low glucose concentration.

This study has shown that adiponectin stimulated insulin secretion without causing Ca^{2+} entry into the cytosol. The following cascade is generally accepted to be involved in glucose-induced insulin secretion. When glucose is metabolised in the cytosol and mitochondria, ATP is generated and promotes the closure of ATP-sensitive potassium channels, thereby depolarising the plasma membrane potential. Depolarisation of the plasma membrane leads to activation of voltage-dependent Ca^{2+} channels, Ca^{2+} entry into the cytosol and a rise in $[Ca^{2+}]_c$, which is thought to finally trigger the exocytosis of insulin-containing granules [29–31]. However, a Ca^{2+}-independent pathway has also been proposed. Thus, Komatsu et al. have suggested that both Ca^{2+}-dependent and Ca^{2+}-independent augmentation occurs via a pathway dependent on glucose metabolism [32, 33]. In this context, we confirmed that adiponectin is able to stimulate insulin secretion when the influx of Ca^{2+} through voltage-dependent Ca^{2+} channels is blocked by nitrendipine; in other words, adiponectin stimulates insulin

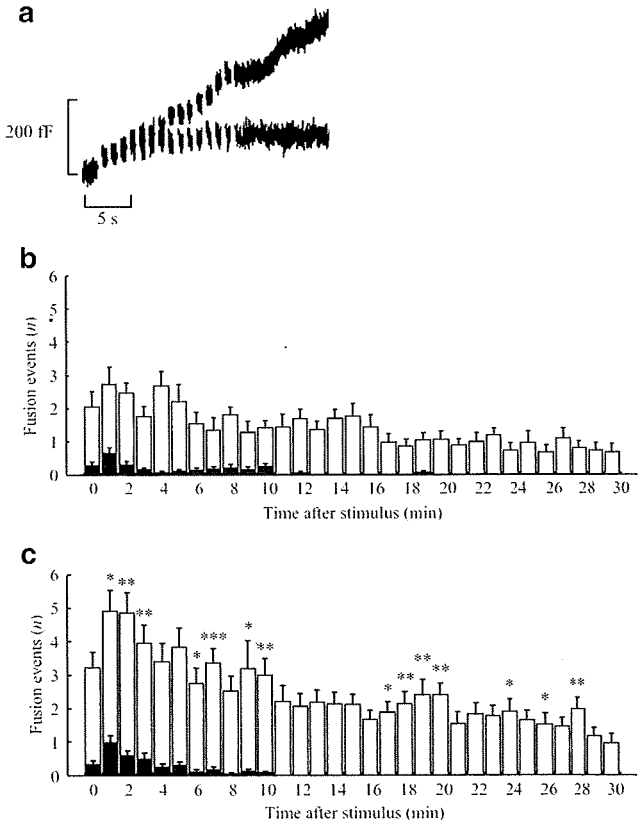

Fig. 4 Adiponectin stimulates insulin release via induction of increased fusion events. **a** The membrane capacitance of mouse beta cells exposed to 5.6 mmol/l glucose alone (lower curve) and 5.6 mmol/l glucose + 10 μg/ml adiponectin (upper curve) cumulatively increased upon repetitive application of depolarising pulses and then plateaued (glucose alone). The traces shown are representative of three experiments. **b**, **c** TIRF images were acquired every 300 ms after the addition of adiponectin. The fusion events per 200 μm^2 were counted manually. Histograms of the number of fusion events in 5.6 mmol/l glucose in the absence (**b**) (n=45) and presence (**c**) (n=52) of adiponectin (10 μg/ml). Black bars, previously docked granules; white bars, newly docked granules. Values are mean±SEM. *p<0.05, **p<0.01, ***p<0.005

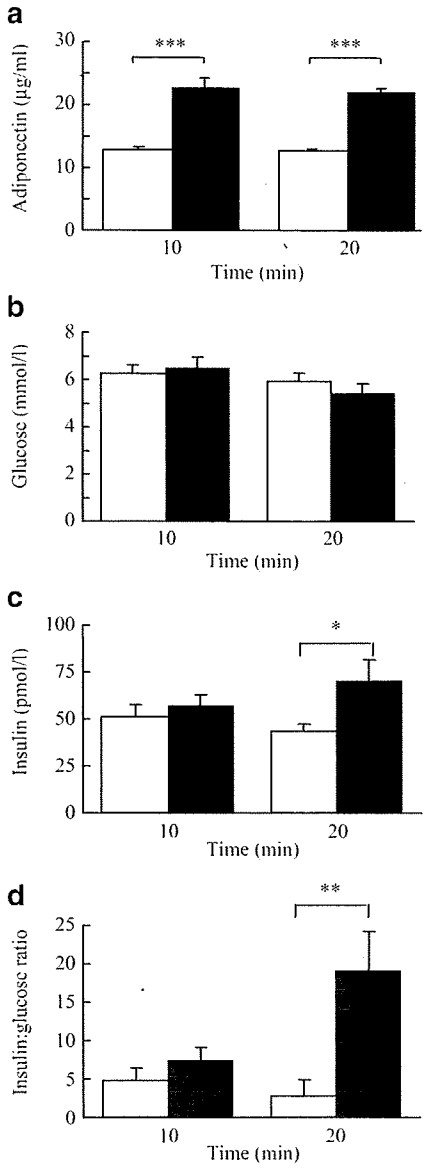

Fig. 5 Adiponectin stimulates insulin secretion in vivo. **a** Plasma adiponectin level after intravenous injection of glucose and saline (white bars, n=8–21) or adiponectin (black bars, n=8–19). **b** Blood glucose and (**c**) plasma insulin levels after the intravenous injections. **d** Ratio of the increment in plasma insulin level to that of blood glucose level after the intravenous injections. Values are means±SEM. *p<0.05, **p<0.01, ***p<0.005

secretion without requiring influx of Ca^{2+} through voltage-dependent Ca^{2+} channels. It may do this through these augmentation pathways triggered by glucose metabolism [33], namely by replacing part of the Ca^{2+}-dependent/ Ca^{2+}-independent augmentation on newly docked granules. In this regard, it should be noted that adiponectin was able to stimulate insulin secretion at 22.2 mmol/l glucose when the influx of Ca^{2+} was blocked by nitrendipine (Fig. 2d). The observation that this stimulation of insulin secretion by adiponectin is relatively small as compared with that of glucose itself under physiological conditions (Fig. 1c) may reflect the relatively small role of the Ca^{2+}-independent augmentation pathway, as suggested by Sato et al. [34].

As another possible mechanism, adiponectin may affect remodelling of the cytoskeleton. The cytoskeleton plays a critical role in glucose-stimulated intracellular trafficking and the exocytosis of insulin-containing granules at the plasma membrane of beta cells. In fact, a previous report showed direct evidence of a dynamic interaction between target membrane soluble *N*-ethylmaleimide-sensitive factor attachment protein receptor protein and F-actin during glucose-stimulated insulin secretion in MIN6 cells [35]. It was recently reported that calpain plays a role in facilitating the actin reorganisation required for glucose-stimulated insulin secretion [36]. Another study has suggested that kinesin I plays an important role in the microfilament-dependent movements of insulin containing granules [37]. Adiponectin may cause direct activation of calpain or kinesin I, to influence remodelling of the cytoskeleton.

Conflicting results on the effects of adiponectin on insulin secretory function in vitro have been reported so far. A previous study showed that while adiponectin decreased glucose/forskolin-induced insulin secretion, it reversed NEFA-induced inhibition of insulin secretion [13]. Another group reported that adiponectin had no effect on either basal or stimulated insulin secretion from human islets [38]. Winzell et al. [39] reported that adiponectin decreases insulin secretion from the pancreatic islets of insulin-resistant mice at a 2.8 mmol/l glucose, but stimulates insulin secretion at 16.7 mmol/l glucose. However, there have been no reports on the effects of adiponectin on insulin secretion in vivo. This study is the first study to demonstrate that adiponectin stimulates insulin secretion not only in vitro, but also in vivo.

In conclusion, we have described a novel effect of adiponectin, namely stimulation of insulin secretion, in addition to its known insulin-sensitising and anti-atherogenic effects. Consequently, adiponectin receptor agonists may be useful in the activation of adiponectin signalling as a new therapeutic strategy for treating diabetes and atherogenic diseases.

Acknowledgements We thank A. Ohyama, C. Kokaki-Kaizuka, N. Kowatari-Otsuka, K. Takasawa and H. Chiyonobu for their excellent technical assistance and mouse husbandry.

Duality of interest The authors declare that there is no duality of interest associated with this manuscript.

References

1. Scherer PE, Williams S, Fogliano M, Baldini G, Lodish HF (1995) A novel serum protein similar to C1q, produced exclusively in adipocytes. J Biol Chem 270:26746–26749
2. Hu E, Liang P, Spiegelman BM (1996) AdipoQ is a novel adipose-specific gene dysregulated in obesity. J Biol Chem 271: 10697–10703

3. Maeda K, Okubo K, Shimomura I, Funahashi T, Matsuzawa Y, Matsubara K (1996) cDNA cloning and expression of a novel adipose specific collagen-like factor, apM1 (AdiPose Most abundant Gene transcript 1). Biochem Biophys Res Commun 221:286–296
4. Nakano Y, Tobe T, Choi-Miura NH, Mazda T, Tomita M (1996) Isolation and characterization of GBP28, a novel gelatin-binding protein purified from human plasma. J Biochem (Tokyo) 120: 803–812
5. Arita Y, Kihara S, Ouchi N et al (1999) Paradoxical decrease of an adipose-specific protein, adiponectin, in obesity. Biochem Biophys Res Commun 257:79–83
6. Yamauchi T, Kamon J, Waki H et al (2001) The fat-derived hormone adiponectin reverses insulin resistance associated with both lipoatrophy and obesity. Nat Med 7:941–946
7. Yamauchi T, Kamon J, Minokoshi Y et al (2002) Adiponectin stimulates glucose utilization and fatty-acid oxidation by activating AMP-activated protein kinase. Nat Med 8:1288–1295
8. Tomas E, Tsao TS, Saha AK et al (2002) Enhanced muscle fat oxidation and glucose transport by ACRP30 globular domain: acetyl-CoA carboxylase inhibition and AMP-activated protein kinase activation. Proc Natl Acad Sci U S A 99:16309–16313
9. Fruebis J, Tsao TS, Javorschi S et al (2001) Proteolytic cleavage product of 30-kDa adipocyte complement-related protein increases fatty acid oxidation in muscle and causes weight loss in mice. Proc Natl Acad Sci U S A 98:2005–2010
10. Kubota N, Terauchi Y, Yamauchi T et al (2002) Disruption of adiponectin causes insulin resistance and neointimal formation. J Biol Chem 277:25863–25866
11. Yamauchi T, Kamon J, Ito Y et al (2003) Cloning of adiponectin receptors that mediate antidiabetic metabolic effects. Nature 423:762–769
12. Kharroubi I, Rasschaert J, Eizirik DL, Cnop M (2003) Expression of adiponectin receptors in pancreatic beta cells. Biochem Biophys Res Commun 312:1118–1122
13. Rakatzi I, Mueller H, Ritzeler O, Tennagels N, Eckel J (2004) Adiponectin counteracts cytokine- and fatty acid-induced apoptosis in the pancreatic beta-cell line INS-1. Diabetologia 47:249–258
14. Lacy PE, Malaisse WJ (1973) Microtubules and beta cell secretion. Recent Prog Horm Res 29:199–228
15. Eto K, Tsubamoto Y, Terauchi Y et al (1999) Role of NADH shuttle system in glucose-induced activation of mitochondrial metabolism and insulin secretion. Science 283:981–985
16. Schuit F, De Vos A, Farfari S et al (1997) Metabolic fate of glucose in purified islet cells. Glucose-regulated anaplerosis in beta cells. J Biol Chem 272:18572–18579
17. Malaisse WJ, Sener A (1987) Glucose-induced changes in cytosolic ATP content in pancreatic islets. Biochim Biophys Acta 927:190–195
18. Gopel S, Zhang Q, Eliasson L et al (2004) Capacitance measurements of exocytosis in mouse pancreatic alpha-, beta-, and delta-cells within intact islets of Langerhans. J Physiol 556:711–726
19. Gillis KD (1995) Single-channel recording. Plenum, New York, pp 155–197
20. Kanno T, Ma X, Barg S et al (2004) Large dense-core vesicle exocytosis in pancreatic beta-cells monitored by capacitance measurements. Methods 33:302–311
21. Ohara-Imaizumi M, Nakamichi Y, Tanaka T, Ishida H, Nagamatsu S (2002) Imaging exocytosis of single insulin secretory granules with evanescent wave microscopy: distinct behavior of granule motion in biphasic insulin release. J Biol Chem 277: 3805–3808
22. Ohara-Imaizumi M, Nishiwaki C, Kikuta T, Nagai S, Nakamichi Y, Nagamatsu S (2004) TIRF imaging of docking and fusion of single insulin granule motion in primary rat pancreatic beta-cells: different behaviour of granule motion between normal and Goto-Kakizaki diabetic rat beta-cells. Biochem J 381:13–18
23. Vives-Pi M, Somoza N, Fernandez-Alvanrez J et al (2003) Evidence of expression of endotoxin receptors CD14, toll-like receptors TLR4 and TLR2 and associated molecule MD-2 and of sensitivity to endotoxin (LPS) in islet beta cells. Clin Exp Immunol 133:208–218
24. Eddlestone GT, Oldham SB, Lipson LG, Premdas FH, Beigelman PM (1985) Electrical activity, cAMP concentration, and insulin release in mouse islets of Langerhans. Am J Physiol 248:C145–C153
25. Ikeda Y, Iguchi H, Nakata M et al (2005) Identification of N-arachidonylglycine, U18666A, and 4-andorostene-3, 17-dione as novel insulin secretagogues. Biochem Biophys Res Commun 333:778–786
26. Russell RR 3rd, Bergeron R, Shulman GI, Young LH (1999) Translocation of myocardial GLUT4 and increased glucose uptake through activation of AMPK by AICAR. Am J Physiol 277: H643–H649
27. Kurth-Kraczek EJ, Hirshman MF, Goodyear LJ, Winder WW (1999) 5′ AMP-activated protein kinase activation causes GLUT4 translocation in skeletal muscle. Diabetes 48:1667–1671
28. da Silva Xavier G, Leclerc I, Varadi A, Tsuboi T, Moule SK, Rutter GA (2003) Role for AMP-activated protein kinase in glucose-stimulated insulin secretion and preproinsulin gene expression. Biochem J 371:761–774
29. Ashcroft FM, Proks P, Smith PA, Ammala C, Bokvist K, Rorsman P (1994) Stimulus-secretion coupling in pancreatic beta cells. J Cell Biochem 55:54–65
30. Dukes ID, Philipson LH (1996) K^+ channels: generating excitement in pancreatic beta-cells. Diabetes 45:845–853
31. Wollheim CB, Lang J, Regazzi R (1996) The exocytotic process of insulin secretion and its regulation by Ca^{2+} and G-proteins. Diabetes Rev 4:276–297
32. Komatsu M, Schermerhorn T, Aizawa T, Sharp GW (1995) Glucose stimulation of insulin release in the absence of extracellular Ca^{2+} and in the absence of any increase in intracellular Ca^{2+} in rat pancreatic islets. Proc Natl Acad Sci U S A. 92:10728–10732
33. Komatsu M, Noda M, Sharp GW (1998) Nutrient augmentation of Ca^{2+}-dependent and Ca^{2+}-independent pathways in stimulus-coupling to insulin secretion can be distinguished by their guanosine triphosphate requirements: studies on rat pancreatic islets. Endocrinology 139:1172–1183
34. Sato Y, Nenquin M, Henquin JC (1998) Relative contribution of Ca^{2+}-dependent and Ca^{2+}-independent mechanisms to the regulation of insulin secretion by glucose. FEBS Lett 421:115–119
35. Thurmond DC, Gonelle-Gispert C, Furukawa M, Halban PA, Pessin JE (2003) Glucose-stimulated insulin secretion is coupled to the interaction of actin with the t-SNARE (target membrane soluble N-ethymaleimide-sensitive factor attachment protein receptor protein) complex. Mol Endocinol 17:732–742
36. Turner MD, Fulcher FK, Jones CV et al (2007) Calpain facilitates actin reorganization during glucose-stimulated insulin secretion. Biochem Biophys Res Commun 352:650–655
37. Varadi A, Tsuboi T, Johnson-Cadwell LI, Allan VJ, Rutter GA (2003) Kinesin I and cytoplasmic dynein orchestrate glucose-stimulated insulin-containing vesicle movements in clonal MIN6 beta-cells. Biochem Biophys Res Commun 311:272–282
38. Staiger K, Stefan N, Staiger H et al (2005) Adiponectin is functionally active in human islets but does not affect insulin secretory function or beta-cell lipoapoptosis. J Clin Endocrinol Metab 90:6707–6713
39. Winzell MS, Nogueiras R, Dieguez C, Ahren B (2004) Dual action of adiponectin on insulin secretion in insulin-resistant mice. Biochem Biophys Res Commun 321:154–160

J Pharmacol Sci 106, 627 – 638 (2008)

Journal of Pharmacological Sciences

Full Paper

Peroxisome Proliferator-Activated Receptor γ (PPARγ) Suppresses Colonic Epithelial Cell Turnover and Colon Carcinogenesis Through Inhibition of the β-Catenin / T Cell Factor (TCF) Pathway

Toshio Fujisawa[1,†], Atsushi Nakajima[1,2,†], Nobutaka Fujisawa[1], Hirokazu Takahashi[1], Ikuko Ikeda[1], Ayako Tomimoto[1], Kyoko Yonemitsu[1], Noriko Nakajima[3], Chiho Kudo[4], Koichiro Wada[4,*], Naoto Kubota[5], Yasuo Terauchi[6], Takashi Kadowaki[5], Hitoshi Nakagama[7], and Richard S. Blumberg[2]

[1]*Division of Gastroenterology, and [6]Division of Endocrinology and Metabolism, Yokohama City University School of Medicine, 3-9 Fuku-ura, Kanazawa-ku, Yokohama 236-0004, Japan*
[2]*Gastroenterology Division, Brigham and Women's Hospital, Harvard Medical School, 75 Francis Street, Boston, MA 02115, USA*
[3]*Department of Pathology, National Institute of Infectious Diseases, 1-23-1 Toyama, Shinjuku-ku, Tokyo 162-8640, Japan*
[4]*Department of Pharmacology, Graduate School of Dentistry, Osaka University, 1-8 Yamadaoka, Suita, Osaka 565-0871, Japan*
[5]*Department of Metabolic Diseases, Graduate School of Medicine, University of Tokyo, 7-3-1 Hongo, Bunkyo-ku, Tokyo 113-0033, Japan*
[7]*Biochemistry Division, National Cancer Center Research Institute, 1-1 Tsukiji 5-chome, Chuo-ku, Tokyo 104-0045, Japan*

Received October 4, 2007; Accepted February 20, 2008

Abstract. Peroxisome proliferator-activated receptor γ (PPARγ), a nuclear receptor superfamily member, plays a major role in lipid metabolism and insulin sensitivity. We investigated the role of PPARγ in colonic epithelial cell turnover and carcinogenesis in colon because PPARγ is strongly expressed in colonic epithelium. Administration of PPARγ agonists suppressed epithelial cell turnover in mice. Expression level of β-catenin protein, a key molecule in carcinogenesis, was increased in mouse colon treated with PPARγ ligands. A direct interaction between β-catenin and PPARγ in cultured cell lines and colonic epithelium in mice was observed. Ligand-activated PPARγ ligand directly interacts with β-catenin, retaining it in the cytosol and reducing β-catenin / T cell factor (TCF) transcriptional activity that is functionally important on aberrant crypt foci (ACF) formation. PPARγ hetero-deficiency promoted the induction of ACF, but had no effect on the incidence of colonic polyps. These results indicate that PPARγ regulates colonic epithelial cell turnover via direct interactions with β-catenin, resulting in inhibition of β-catenin–mediated transcriptional pathways that are involved in promoting cell proliferation. Our findings suggest that PPARγ plays a role as a physiological regulator of colonic epithelial cell turnover and consequently predisposition to the development of colon cancer in early stage.

Keywords: peroxisome proliferator-activated receptor γ (PPARγ), epithelial cell turnover, β-catenin, colon cancer

Introduction

Peroxisome proliferator-activated receptor γ (PPARγ), a nuclear receptor superfamily member, is strongly expressed in adipocytes (1, 2) and plays a major role in lipid metabolism (3 – 5) and insulin sensitivity (6, 7). It has been demonstrated that 15-deoxy-Δ12,14-prostaglandin J2 (15d-PGJ_2) is a potential endogenous ligand (8) and that thiazolidinediones (TZD), such as pioglitazone and rosiglitazone, widely used as oral hypoglycemic agents, are specific exogenous ligands for PPARγ. PPARγ has also been reported to be expressed in the intestinal epithelium (9). In intestinal epithelium,

†These authors contributed equally to this work.
*Corresponding author. kwada@dent.osaka-u.ac.jp
Published online in J-STAGE on April 5, 2008 (in advance)
doi: 10.1254/jphs.FP0071766

PPARγ has been suggested to play an important role as an endogenous inhibitor of NF-κB–mediated inflammation (10). PPARγ has also been detected in colon cancer cells where it has been indirectly linked to colon cancer pathogenesis (11). However, the relationship between PPARγ and colon cancer have been contradictory. The groups of Lefebvre et al. and Saez et al. have shown that treatment with PPARγ ligands enhances colon carcinogenesis in APC^{Min} mice (12, 13). In contrast, Sarraf et al. have demonstrated that troglitazone and rosiglitazone suppress the growth of human colonic cancer cells (14). We previously conducted a study to clarify these controversial results and demonstrated that PPARγ ligands significantly suppress colon carcinogenesis in the azoxymethane (AOM)-induced colon cancer model (15). PPARγ ligands also significantly reduced the incidence of aberrant crypt foci (ACF), a putative precancerous lesion, and reduced the incidence of tumors developing in the colon in this model. In addition, Tanaka et al. also reported on the suppressive effect of PPARγ ligands on the formation of ACF in the AOM-induced colon cancer model in rats (16). Niho et al. demonstrated that PPARγ ligands suppress tumor formation in APC^{Min} mice (17, 18). These results, including our own report, indicate that activation of PPARγ by various ligands suppresses colon carcinogenesis at the initiation, promotion, and progression stages of the disease. However, the molecular mechanisms underlying the suppression of colonic carcinogenesis by PPARγ activation have not yet been clarified.

It has been reported that the β-catenin–Wnt signaling pathway controls cell proliferation and body patterning throughout development (19). In addition, β-catenin plays an important role as a transcriptional activator in colonic carcinogenesis (20 – 22). Specifically, accumulation of β-catenin in the cytosol results in its nuclear translocation in the presence of active Wnt signaling, leading to induction of a genetic program that is involved in the promotion of cell growth at the initiation of colonic carcinogenesis (23, 24). Thus, given the effects of PPARγ ligands on inhibiting the development of ACF and the direct role of Wnt-β–catenin pathways in mediating ACF formation (25), we hypothesized that PPARγ might affect β-catenin–mediated transcriptional regulation as a mechanism to inhibit colon carcinogenesis. Consistent with this, Girnun et al. showed an increase in the levels of β-catenin in the colonic epithelium of PPARγ hetero–deficient mice (26), and concluded that PPARγ suppresses colonic carcinogenesis by regulating the expression levels of β-catenin. However these studies do not show a direct relationship between PPARγ and β-catenin. Namely, the relationship between PPARγ and β-catenin in colon carcinogenesis remains unclear. The aim of this study was, therefore, to clarify the direct interaction between PPARγ and β-catenin in colon carcinogenesis. To clarify the direct interaction between PPARγ and β-catenin may reveal the exact role of PPARγ in influencing epithelial cell turnover and the initial stages of colonic carcinogenesis because β-catenin is the key molecule in the carcinogenesis. Here, we observed that PPARγ directly interacts with β-catenin and diminishes the translocation of β-catenin into the nucleus, which suppresses the activity of β-catenin in mediating its transcriptional program on culture cells and the AOM-induced colon cancer model.

Materials and Methods

Cell lines and culture conditions

HT-29, Lovo, Caco2, and DLD1 cells were purchased from the Japanese Collection of Research Bioresources (Osaka). HT-29 cells were maintained in D-MEM medium supplemented with 10% fetal bovine serum, 200 U/ml of penicillin, and 200 μg of streptomycin. Lovo cells were maintained in McCoy's 5A medium supplemented with 20% fetal bovine serum, 200 U/ml of penicillin, and 200 μg of streptomycin.

Reagents

Pioglitazone and rosiglitazone were kindly provided by Takeda Chemical (Osaka) and by SmithKline Beecham (West Sussex, UK), respectively. PGJ_2 was purchased from ALEXIS Biochemicals (Lausen, Switzerland).

BrdU and PCNA assay

Bromodeoxyuridine (BrdU; BD Biosciences, Franklin Lakes, NJ, USA) was used to label the colonic epithelial cells undergoing DNA replication. BrdU was diluted in phosphate-buffered saline at 1 mg/ml and used at 50 mg /kg body weight. It was given intraperitoneally 1 h prior to the sacrifice of the animals. The immunohistochemical detection of BrdU was conducted using a commercial kit (BD Biosciences). Proliferating cell nuclear antigen (PCNA) was also used to label the colonic epithelial cells undergoing DNA replication and the immunohistochemical detection of PCNA was conducted using a commercial kit (Zymed Laboratories Inc., South San Francisco, CA, USA).

Reporter assay

Lovo cells were seeded at a density of 1×10^4 cells/well in 24-well plates and cultured for 24 h, prior to transfection. Transfections were performed in accordance with the manufacturer's procedure using 3 μl of Lipofectamine 2000 (Invitrogen, Carlsbad, CA, USA),

2 μg of Firefly Luciferase Reporter DNA (TOPflash or control FOP flash; Upstate Biotechnology, Inc., New York, NY, USA), and 0.5 μg of phRL-TK-Renilla Luciferase (Promega, Madison, WI, USA) as a control for transfection efficiency in 200 μl of Opti-mem (Invitrogen). At 24 h after the transfection, the medium was removed and the cells were treated with medium containing or not containing 10 μM of PGJ_2 for 8 h. The medium was removed and the Firefly and Renilla luciferase activities were sequentially measured using the Dual-Glo buffer system (Promega). Transfections were performed in triplicate and repeated five times for each set. To normalize the data, the Firefly luciferase activity in each well was divided by the Renilla luciferase value. Each experiment was repeated at least three times. Data represent the TOP/FOP relative luciferase activity and the mean ± S.D. from three independent experiments.

Knockdown of PPARγ using siRNA

PPARγ siRNA was purchased from Santa Cruz Biotechnology (Santa Cruz, CA, USA). This siRNA was transfected into 70%-confluent Lovo cells using Lipofectamine 2000. The cells were treated with 12 nM of PPARγ siRNA for 24 h prior to the reporter assay. The Stealth RNAi Negative Control Medium GC (Invitrogen) was used as the negative control.

Reverse transcription-polymerase chain reaction (RT-PCR)

Total RNA was isolated from the cells using the RNAeasy Kit (Qiagen, Valencia, CA, USA). First-strand cDNA was prepared and RT-PCR was performed using the RNA PCR kit (Takara, Otsu). The PCR primers were designed according to the reported sequences as follows: c-myc (ref. 27) (forward 5'-GGTCTTCCCCTACCCT CTCAACGA-3', reverse 5'-GGCAGCAGGATAGTCC TTCCGAGT-3'), cyclin D1 (ref. 28) (forward 5'-TGT GCTGCGAAGTGGAAACC-3', reverse 5'-AAATCG TGCGGGGTCATTGC-3'), β-actin (ref. 27) (forward 5'-AAGAGAGGCATCCTCACCCT-3', reverse 5'-TAC ATGGCTGGGGTGTTGA-3'). After initial denaturation for 10 min at 9°C, the reaction was conducted over 20 PCR cycles of 95°C for 60 s and 56°C for 60 s. β-Actin mRNA quantification was also performed for standardization.

Immunoprecipitation

Cell extracts were prepared in lysis buffer (20 mM HEPES, 2 mM EGTA, 50 mM β-glycerophosphate, 10% glycerol, 1% Triton X-100, 1 mM dithiothreitol, 1 mM vanadate, and 0.04 mM phenylmethylsulfonyl fluoride) containing a cocktail of protease inhibitors (Sigma, St. Louis, MO, USA). To determine the interaction between PPARγ and β-catenin in various colon cancer cell lines in the presence or absence of PPARγ ligands, immunoprecipitation was performed using a specific anti-PPARγ antibody (Santa Cruz Biotechnology) or anti-β-catenin antibody (BD Transduction Laboratories, Lexington, KY, USA). The antibodies were pre-adsorbed on protein G-Sepharose beads for 1 h at 4°C. Equal amounts of cell extracts (400 μg protein each) were incubated with the respective antibody-crosslinked beads overnight at 4°C, with purification of the antibody-protein complex beads by centrifugation. The samples were then resolved by SDS-PAGE, followed by Western blotting. The signals were detected with an ECL-plus kit (Amersham Pharmacia Biotech, London, UK) in accordance with the manufacturer's protocol.

GST-PPARγ fusion protein and GST pull-down assay

The full-length human PPARγ1 cDNA was subcloned into the pGEX-4T vector (Amersham Pharmacia Biotech). The GST-PPARγ fusion protein was synthesized and purified using the B-PER GST Fusion Protein Purification Kit (PIERCE, Rockford, IL, USA). A clone of β-catenin (GeneStorm clones: RG001399) was purchased from Invitrogen. In vitro transcription and translation were performed using the TNT kit (Promega) in the presence of [^{35}S]-methionine (Amersham Pharmacia Biotech). Lysates were prepared by solubilizing the cells in immunoprecipitation buffer. The β-catenin synthesized in vitro was pulled down with either the GST-PPARγ fusion protein or the GST protein alone and the immunoprecipitates resolved by SDS-PAGE under reducing conditions, followed by autoradiography.

Animal models

All mice were treated humanely in accordance with the National Institutes of Health and AERI-BBRI Animal Care and Use Committee guidelines. All animal experiments were approved by the institutional Animal Care and Use Committee of Yokohama City University School of Medicine. AOM was purchased from Sigma. Heterozygous PPARγ-deficient [PPARγ (+/−)] mice and wild-type [(PPARγ (+/+)] mice were generated as described previously (29). They were fed a standard diet (Oriental MF; Oriental Co., Tokyo) until sacrifice. Female BALB/c mice were purchased from CLEA Japan (Tokyo). All the animals were housed in a ventilated, temperature-controlled room (23 ± 1°C) under a 12-h light/dark cycle. To prepare the experimental diet, pioglitazone was mixed with the powdered standard diet (Oriental MF) and stored at 4°C until use; the concentration of pioglitazone in the experimental diet was 200 ppm. After acclimatization for 3 days to the housing

environment and the standard diet, the BALB/c mice were divided into groups that were fed either the standard diet or the experimental diet until sacrifice.

Induction of ACF

Eight-week-old PPARγ (+/+) (n = 14) and PPARγ (+/–) (n = 14) mice were injected intraperitoneally with 10 mg/kg of AOM once a week for 2 weeks. Another set of 8-week-old PPARγ (+/+) (n = 14) and PPARγ (+/–) (n = 14) mice were treated with saline as a control. After the first administration of AOM or saline for four weeks, the mice were sacrificed at experimental week 5. The entire colon was immediately removed and fixed, and the numbers of ACF and aberrant crypts (ACs) were counted as described previously (15).

Induction of colonic tumors

Eight-week old PPARγ (+/+) (n = 20) and PPARγ (+/–) (n = 20) mice were injected intraperitoneally with 10 mg/kg of AOM once a week for 6 weeks. All the surviving mice were sacrificed 37 weeks after the last injection of AOM. The colons were removed immediately and fixed in 10% neutralized formalin as described previously (15).

Histological analysis of the ACF and colonic tumors

All the colons were removed and fixed in neutralized 10% formalin overnight at 4°C. To facilitate counting of the ACF and colonic tumors, the colons were stained with 0.2% methylene blue solution and examined under a dissecting microscope. The ACF and colonic tumors were removed and embedded in paraffin blocks in accordance with standard procedures.

Immunohistochemical analysis

Paraffin-embedded sections were deparaffinized and subjected to immunohistochemical staining with an anti-mouse β-catenin monoclonal antibody (BD Transduction Laboratories) using a Vectastain ABC kit (Vector Laboratories, Burlingame, CA, USA) in accordance with the manufacturer's instructions. The primary β-catenin antibody was used at a dilution of 1:800 and the PPARγ antibody at a dilution of 1:500, with nuclear counterstaining performed using hematoxylin.

Immunoblotting and immunofluorescence

Colonic epithelium was isolated and protein extraction performed. Western blotting was performed using anti-PPARγ (Santa Cruz Biotechnology), anti–β-catenin (BD Transduction Laboratories), or anti-G3PDH (Trevigen, Gaithersburg, MD, USA) antibodies. Segments of colonic epithelium from mice fed the experimental or standard diet were embedded in the same block and frozen sections cut. For the immunofluorescence analyses, the frozen tissue sections were incubated in a working solution of M.O.M. Mouse IgG Blocking Reagent (Vector Laboratories) at 37°C for 1 h. The sections were then washed with PBS and incubated in a working solution of M.O.M. Dilute (Vector Laboratories) at room temperature for 30 min. The sections were then exposed to an anti–β-catenin mouse monoclonal antibody (BD Transduction Laboratories) (1:100 diluted with M.O.M. Dilute) or anti-rabbit PPARγ polyclonal antibody (Santa Cruz Biotechnology) (1:10 diluted with M.O.M. Dilute) overnight at 4°C. After washing with PBS, the sections were incubated with Alexa Fluor 488 goat anti-mouse IgG (Molecular Probes, Eugene, OR, USA) or Alexa Fluor 555 goat anti-rabbit IgG (Molecular Probe) at 37°C for 1 h. Imaging was performed using a confocal microscope equipped with an argon-krypton laser (LSM-Micro-System; Carl Zeiss, Oberkochen, Germany). Alexa Fluor 488 dye exhibited green fluorescence and Alexa Fluor 555 dye exhibited red fluorescence. The emission patterns of the two fluorescence labels were collected separately and the data overlaid to generate two-color images.

Statistical analyses

Statistical analyses for ACF and colonic tumor multiplicity were conducted by using the Mann-Whitney *U* test. Other statistical analyses of the differences in the incidence and histologic characteristics of the colonic tumors were performed by Student's *t*-test. Differences were considered significant when P values were <0.05.

Results

PPARγ modulates the levels of β-catenin

To determine the effect of PPARγ on β-catenin levels, we examined the quantities of PPARγ and β-catenin proteins in the colonic epithelium from PPARγ (+/–) and PPARγ (+/+) mice. The results of Western-blot analysis indicated that the PPARγ protein levels were reduced in the colonic epithelium of the PPARγ (+/–) mice as compared to that observed in the colonic epithelium of wild-type mice (Fig. 1A). Interestingly, the β-catenin protein levels in the colonic epithelium of the PPARγ (+/–) mice were also reduced in comparison to that observed in the colonic epithelium of the wild-type mice (Fig. 1B). These results indicate that the expression of PPARγ and β-catenin in the colonic epithelium are coordinately regulated. We, therefore, examined whether PPARγ might upregulate β-catenin levels in the colonic epithelium of PPARγ-ligand–treated mice. As expected, Western-blot analysis showed significant upregulation of β-catenin protein levels in the colonic epithelium of

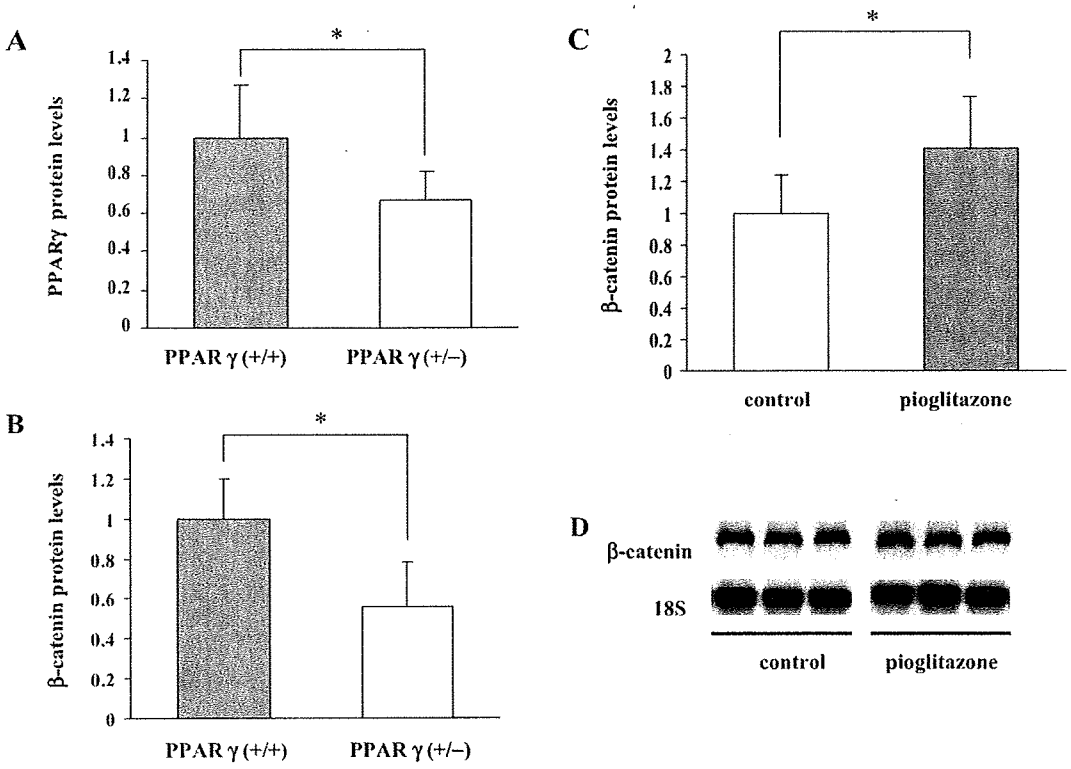

Fig. 1. *β*-Catenin expression in the colonic epithelium of PPARγ (+/–)/(+/+) and TZD-treated mice. A and B: Expression of PPARγ (A) or *β*-catenin (B) in the colonic epithelium of PPARγ (+/–) and PPARγ (+/+) mice. Protein lysates were prepared from the colonic epithelium of five mice per group, and the levels of PPARγ and *β*-catenin were analyzed by Western-blot analysis. The averaged expression of each protein in wild type (PPARγ (+/+)) mice was defined as 1.0. The relative expression level of each protein in the PPARγ (+/–) mice was expressed as "protein level" compared to that in wild type (PPARγ (+/+)) mice. **P*<0.05, as compared with the result in the PPARγ (+/–) mice. C: *β*-Catenin protein levels in the colonic epithelium of BALB/c mice treated with pioglitazone. Protein lysates were prepared from the colonic epithelium of five mice per group and the levels of *β*-catenin were analyzed by Western-blot analysis. The *Y* axis indicates the relative expression levels of *β*-catenin in the control mice. **P*<0.05, as compared with the results in the control mice. D: *β*-Catenin mRNA levels in the colonic epithelium of BALB/c mice treated with pioglitazone. Total RNA was isolated from the colonic epithelium of five mice per group, and the levels of *β*-catenin mRNA were determined by northern blot analysis. Levels of 18S were determined as an internal control. The results of Northern blot analysis indicated no differences in the *β*-catenin mRNA levels between the pioglitazone-treated mice and control mice.

the pioglitazone-treated mice as compared to that detected in the colonic epithelium of the vehicle-treated control mice (Fig. 1C).

To clarify whether the PPARγ-mediated increase in *β*-catenin protein levels was due to a transcriptional-related mechanism, we performed northern blot analysis on RNA from the colonic epithelium of the pioglitazone-treated and control mice. The results of northern blot analysis showed no differences in the *β*-catenin mRNA levels in the colonic epithelium from the pioglitazone-treated and control mice (Fig. 1D). These results indicate that the PPARγ-mediated increase in *β*-catenin protein levels is not due to transcriptional regulation, but rather due to a post-transcriptional event.

Activation of PPARγ by ligand treatment suppresses β-catenin/TCF–mediated transcription in colonic carcinogenesis

It is well known that *β*-catenin which accumulates in the cytosol is translocated into the nucleus whereupon it binds with members of the T cell factor (TCF) / lymphoid enhancing factor (LEF) family and induces target gene transcription, such as c-myc and cyclin D1. To determine whether ligation of PPARγ regulates *β*-catenin /TCF activity, Lovo, a colonic cancer cell line, was transfected with a TCF reporter vector, TOPflash, which contains a combination of TCF-binding elements. Incubation with the PPARγ ligand PGJ_2 significantly suppressed the transcriptional activity of TOPflash (Fig. 2A). In contrast, knockdown of PPARγ protein expression by treatment of Lovo cells with siRNA

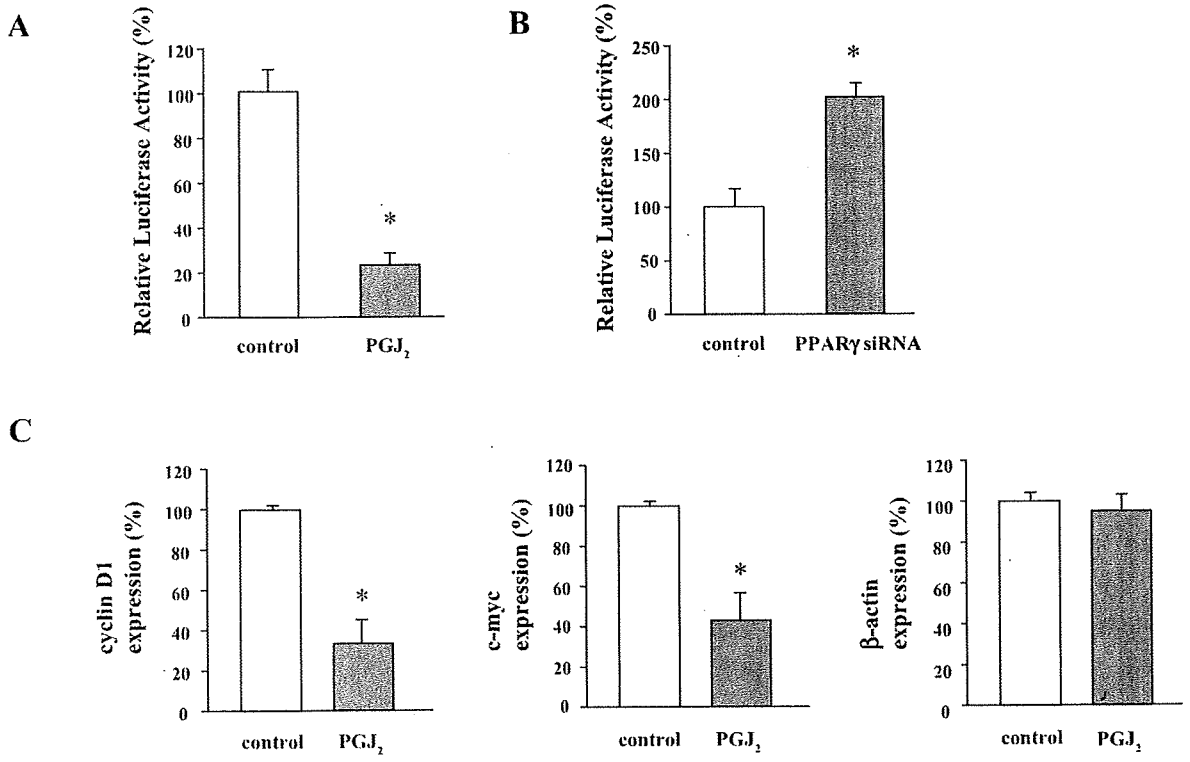

Fig. 2. PPARγ ligand suppresses the β-catenin/TCF–mediated transcription activity in colonic carcinogenesis. A: Ligand activation of PPARγ reduces β-catenin/TCF activity. Lovo cells were transiently transfected with the TCF-responsive promoter TOPflash or FOP flash. After incubation with 10 μM PGJ_2 for 8 h, dual-luciferase assays were performed. B: siRNA inhibition of PPARγ induces β-catenin/TCF activity. Lovo cells were treated with 12 nM PPARγ siRNA for 24 h before performing the reporter assay. Each experiment was repeated at least three times. Data represent the TOPflash/FOP flash relative luciferase activity, and each reported value is the mean ± S.D. from three independent experiments. C: Ligand activation of PPARγ suppresses expression of the β-catenin/TCF target genes c-myc and cyclin D1. Lovo cells were treated with 10 μM PGJ_2 for 5 h. The levels of c-myc and cyclin D1 mRNA were determined by RT-PCR analysis. The level of β-actin as an internal control was also determined. *$P<0.05$, as compared with the result in the control mice.

promoted TOPflash transcriptional activity (Fig. 2B). These results indicate that PPARγ negatively regulates the transcriptional activity of β-catenin/TCF. We then performed RT-PCR to determine whether the PPARγ ligand PGJ_2 regulates expression of β-catenin and TCF target genes. The PPARγ ligand significantly inhibited the expression of c-myc and cyclin D1 (Fig. 2C). Taken together, these results indicate that activation of PPARγ significantly suppresses β-catenin/TCF activity in vitro despite increased levels of β-catenin.

PPARγ directly interacts with β-catenin

To elucidate the mechanism by which activation of PPARγ suppresses the activation of β-catenin and TCF, we investigated the interaction between PPARγ and β-catenin both in vivo and in vitro. Immunoprecipitation of cell extracts from various colonic cancer cell lines with a PPARγ-specific antibody revealed a direct interaction between PPARγ and β-catenin which was increased by treatment with the PPARγ ligand pioglitazone (Fig. 3: A and B). Similar results were observed in the colonic epithelium of mice treated with the PPARγ ligand in vivo (Fig. 3C). In addition, a GST pull-down assay confirmed the direct interaction between PPARγ and β-catenin (Fig. 3D). These data indicate that activation of PPARγ causes it to interact with β-catenin which, in turn, is associated with inhibition of β-catenin translocation into the nucleus. This inhibition of β-catenin translocation into the nucleus is further associated with suppression of the ability of β-catenin and TCF to regulate its normal transcriptional program of activity.

To confirm the direct interaction of PPARγ with β-catenin in vivo, we investigated the localization of PPARγ and β-catenin in the colonic epithelium of mice. As shown in Fig. 4 (A and B), β-catenin was mostly localized to the cell membrane with PPARγ localizing to the nucleus in the crypt of the colon. However, in the surface epithelium, PPARγ and β-catenin co-localized

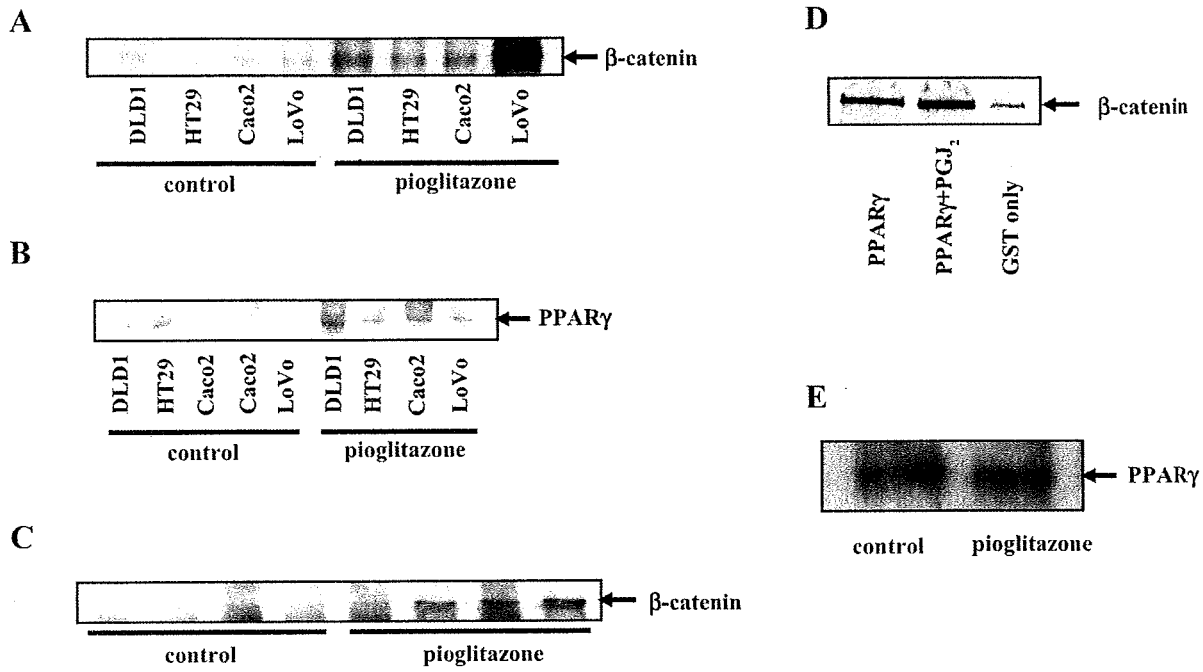

Fig. 3. PPARγ directly associates with β-catenin both in vivo and in vitro. A: Soluble extracts from several colon cancer cells treated/not treated with pioglitazone were immunoprecipitated with anti-PPARγ antibody, as indicated. The presence of β-catenin in the immunoprecipitates was determined by Western blotting with anti–β-catenin antibody. B: Soluble extracts from several colon cancer cells treated/not treated with pioglitazone were immunoprecipitated with anti–β-catenin antibody, as indicated. The presence of PPARγ in the immunoprecipitates was determined by Western blotting with anti-PPARγ antibody. C: Soluble extracts of colonic epithelial cells of BALB/c mice treated/not treated with pioglitazone were immunoprecipitated with anti-PPARγ antibody, as indicated. The presence of β-catenin proteins in the immunoprecipitates was determined by Western blotting with anti–β-catenin antibody. D: β-Catenin–containing plasmids were transcript and translated in vitro in the presence of ^{35}S, and radiolabel proteins were incubated with either GST alone or GST-PPARγ fusion protein. The bindings were assayed in the presence or absence of the specific ligand PGJ_2. The protein complexes formed were pulled down with glutathione-Sepharose beads and resolved by SDS-PAGE, followed by autoradiography. E: Confirmation of PPARγ protein levels treated with or without pioglitazone in Lovo cells. No marked difference was observed.

with each other in the cytosol (Fig. 4C). These data indicate that PPARγ directly interacts with β-catenin, retaining the latter in the cytosol and preventing its transcriptional activity in the nucleus. Taken together, activation of PPARγ by its ligand upregulates the direct interaction between PPARγ and β-catenin in the colonic epithelial cells, suppressing β-catenin translocation into the nucleus. Furthermore, our data suggest that natural PPARγ ligands are more highly expressed in surface epithelium at steady-state.

PPARγ ligand suppresses colonic epithelial cell proliferation

To clarify the mechanism underlying the inhibitory effect of PPARγ on β-catenin transcriptional activity, we investigated the effect of a PPARγ ligand on colonic epithelial cell proliferation in vivo. To do so, we used both BrdU and PCNA labeling for the quantitation of cell proliferation. BrdU is a modified pyrimidine analogue that is readily incorporated into nuclei during the DNA synthetic phase of the cell cycle (S-phase). PCNA is a nuclear antigen whose expression increases during the G_1-phase, peaks at the S-phase, and declines during the G_2/M-phases of the cell cycle. The BrdU-labeled tissue sections and the number of BrdU-labeled cells are shown in Fig. 5 (A – D). The number of BrdU-labeled cells per crypt in the distal colon of pioglitazone-treated mice was significantly reduced as compared with that observed in the colonic epithelium of the control, untreated mice (Fig. 5D). BrdU-stained cells in the colonic epithelium of the pioglitazone- or rosiglitazone-treated mice were decreased and mainly detectable near the crypt base. In contrast, in control mice, BrdU-positive cells extended up from the base towards the surface epithelium. Furthermore, treatment of mice with pioglitazone and rosiglitazone resulted in significantly shorter lengths of the crypts in comparison to control mice (Fig. 5: A – C).

Similarly, the PCNA-labeling index in the colonic epithelium of mice treated with pioglitazone and

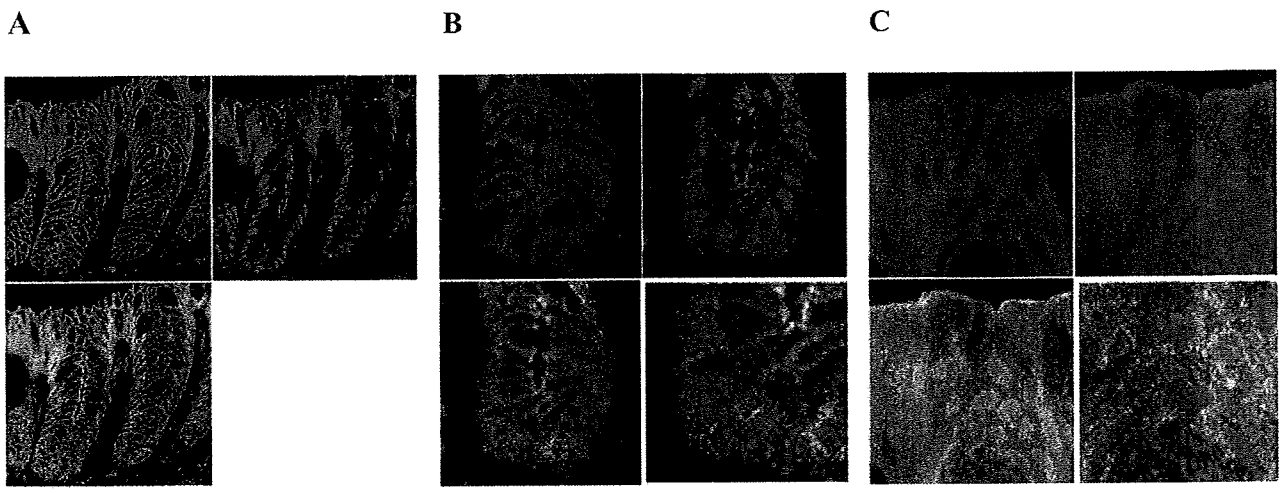

Fig. 4. Immunofluorescence microscopy of PPARγ and β-catenin in the colonic epithelium of BALB/c mice. Immunostaining for PPARγ (Alexa Fluor 488, green) and β-catenin (Alexa Fluor 555, red). A: An entire crypt (magnification = 40). B: The bottom of a crypt (magnification = 62). C: The top of a crypt (magnification = 62). Right bottom corner in (B) and (C) represents a high magnification picture.

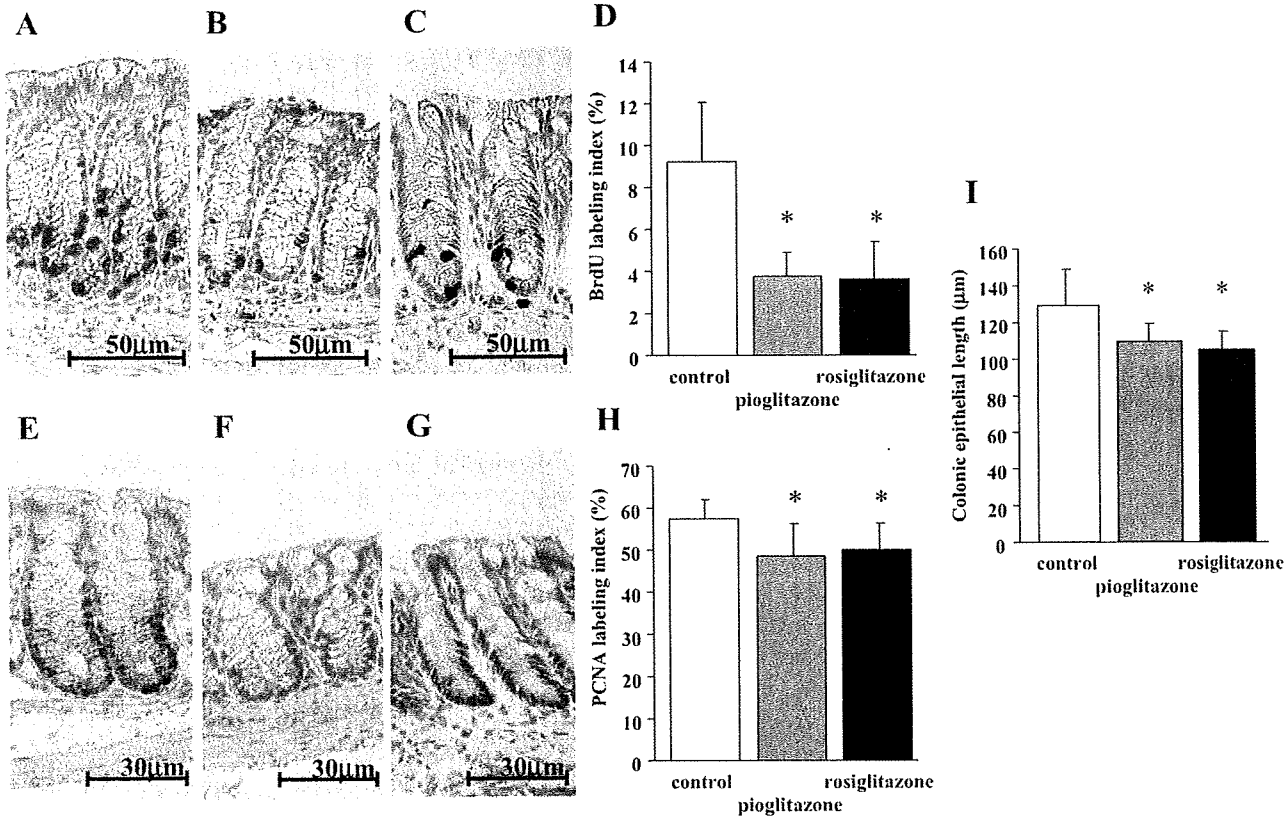

Fig. 5. PPARγ ligand suppresses colonic epithelial cell proliferation. Immunohistochemical staining of BrdU in the colonic epithelium of control mice (A), pioglitazone-treated mice (B), and rosiglitazone-treated mice (C). D: BrdU-labeling index in pioglitazone-treated, rosiglitazone-treated, and control mice. Immunohistochemical staining of PCNA in the colonic epithelium of control mice (E), pioglitazone-treated mice (F), and rosiglitazone-treated mice (G). H: PCNA-labeling index in pioglitazone-treated, rosiglitazone-treated, and control mice. I: Comparison of the colonic epithelial length in pioglitazone-treated, rosiglitazone-treated, and control mice. The colonic epithelial length in the TZD-treated mice was significantly shorter than that in the control mice. *P<0.05 as compared with the results in control mice.

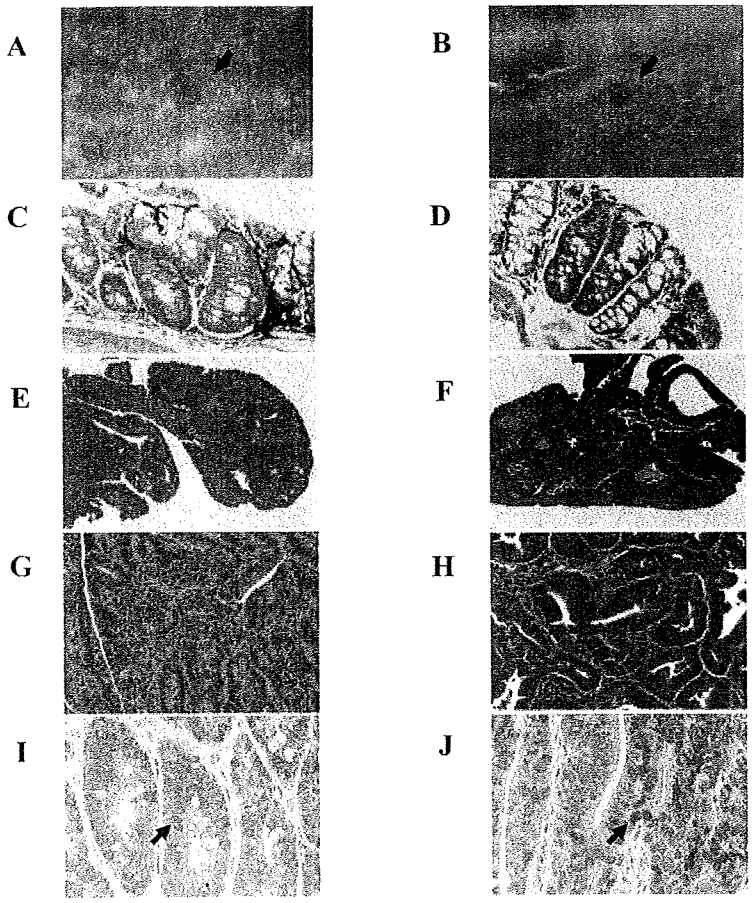

Fig. 6. Histology of ACF and colonic tumors arising in the mice after AOM treatment. ACF arising in the colons of PPARγ (+/–) (A, C) and PPARγ (+/+) (B, D) mice. A and B: 0.2% metylene blue staining: ACF is indicated by the solid arrow; C and D: H & E staining (magnification = ×20). Colonic tumors arising in the colons of PPARγ (+/–) (E, G) and PPARγ (+/+) (F, H) mice. E and F: H & E staining (magnification = ×10). G and H: H & E staining (magnification = ×40). Immunohistochemical staining of β-catenin in the adenomas of PPARγ (+/–) (I) and PPARγ (+/+) (J) mice. β-Catenin was detectable in the cytosol and nuclei (arrows) in the adenomas of both groups of animals

rosiglitazone was also significantly reduced in comparison to that observed in the control mice (Fig. 5: E – H). Importantly, the apoptotic index of the colonic epithelium as determined by TUNEL staining was unchanged in the pioglitazone-treated and control mice (data not shown). These results indicate that PPARγ ligands suppress colonic epithelial cell proliferation and turnover.

Heterozygous PPARγ-deficiency promotes ACF formation in AOM-induced colon carcinogenesis

To investigate the effect of PPARγ-mediated inhibition of β-catenin transcriptional activity in colon carcinogenesis in vivo, we examined the formation of ACF in the AOM-induced colon cancer model in PPARγ (+/–) mice (Fig. 6: A and B). AOM treatment of PPARγ (+/–) mice resulted in a significant increase in the formation of ACF in the colon in comparison to that observed in the colons of wild-type mice similarly treated with AOM (Table 1). However, PPARγ heterodeficiency did not result in an increased incidence or multiplicity of adenocarcinomas (Table 1). Histological analysis of the tumors from both genotypes of mice identified them as either adenomas or adenocarcinomas. Moreover, there were no significant differences in the histologic characteristics of the ACF, adenomas, or adenocarcinomas observed in PPARγ (+/–) mice and PPARγ (+/+) mice (Fig. 6: C – H). As expected, β-catenin was detectable in the cytosol and nuclei in the adenomas of both groups of animals (Fig. 6: I and J). Figure 7 shows that the survival of PPARγ (+/–) mice and PPARγ (+/+) mice was identical and observed to be 85% at 37 weeks.

Discussion

The development of colon cancer is the consequence of a multi-step process (30). This genetically driven program causes cellular hyper-proliferation of normal colonic epithelium, resulting in formation of adenomas and, consequently, carcinomas (31 – 34). In addition, this process is enhanced by chronic inflammation (35). Since PPARγ is regulated by and, in turn, regulated cellular proliferation and inflammation (36, 37), it is of significant importance to the pathogenesis of colon cancer. However, the physiological role of this receptor in the colonic epithelium remains incompletely charac-

Table 1. Effect of PPARγ heterodeficiency on the formation of (a) ACF and (b) colonic tumors in the AOM-induced colon cancer model

a

Genotype	AOM	n	No. of ACF/mouse	No. of ACs/mouse
PPARγ (+/+)	+	14	11.71 ± 5.44	18.21 ± 8.62
PPARγ (+/–)	+	14	16.21 ± 4.28*	26.00 ± 6.00*
PPARγ (+/+)	–	14	0	0
PPARγ (+/–)	–	14	0	0

b

Experimental group	Incidence (%)	Histology			Multiplicity
		Ad	AdCa	total	
PPARγ (+/+)	10/19 (53)	7	17	24	1.26 ± 1.81
PPARγ (+/–)	11/17 (65)¶	6	13	19	1.12 ± 1.10¶

*$P<0.05$, as compared with the results in the PPARγ (+/+) mice treated with AOM. ¶No difference in the number of colon tumors arising in the colons of PPARγ (+/+) and PPARγ (+/–). ACs, aberrant crypts; Ad, adenoma; AdCa, adenocarcinoma.

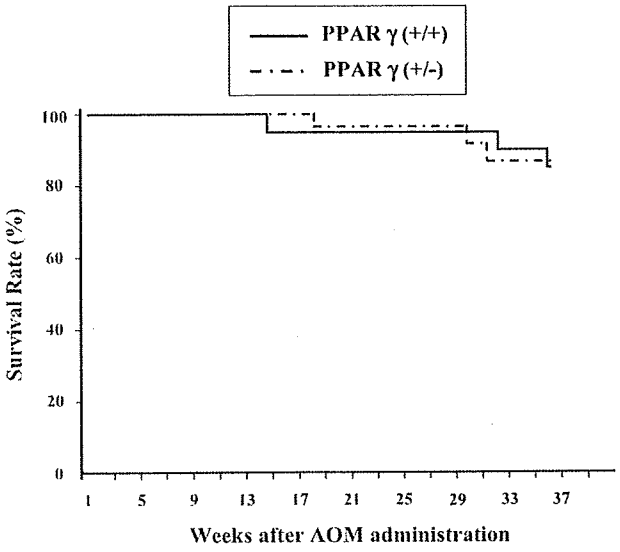

Fig. 7. Survival of PPARγ (+/–) and PPARγ (+/+) mice after AOM treatment. PPARγ (+/–) and PPARγ (+/+) mice were treated with 10 mg/kg of AOM and observed until 37 weeks after AOM administration. There was no significant difference in the survival rates between the two groups.

terized. In addition, it is still unknown how PPARγ affects the cell turnover in colon.

In the present study, we observed that PPARγ ligand markedly suppressed colonic epithelial cell proliferation, independently of apoptosis, resulting in decreased colonic crypt length. These results may indicate that activation of PPARγ induces a cellular program that decreases epithelial cell proliferation. Namely, PPARγ negatively regulates colonic epithelial cell turnover by affecting cell cycle kinetics rather than inducing apoptosis under physiological conditions in vivo. In fact, PPARγ is expressed abundantly in the colonic epithelium, and it is suggested that PPARγ is a key molecule in the regulation of colonic epithelial cell turnover.

To clarify how PPARγ affects the epithelial cell turnover, we investigated the interaction between PPARγ and β-catenin because β-catenin is a key molecule in cell proliferation and ACF formation in the colon (25). We showed that PPARγ activation leads to increased β-catenin protein levels in the colonic epithelium. However, this PPARγ mediated increase in β-catenin protein expression in the colonic epithelium was not associated with the nuclear translocation of β-catenin. Furthermore, it was observed that PPARγ directly interacted with β-catenin in both colonic cancer cell lines and native colonic epithelial cells in vivo and that this interaction was enhanced by treatment with PPARγ ligands, suggesting that binding of β-catenin by PPARγ may prevent its degradation. Moreover, the increase in the direct binding of PPARγ to β-catenin observed here was associated with the decreased β-catenin translocation into the nucleus, despite increased protein levels, and inhibition of β-catenin and TCF dependent transcription.

It has been reported that ligation and activation of PPARγ in HT-29 and Lovo colon cancer cells significantly suppresses cellular proliferation (38). Consistent with this, we observed that PPARγ activation suppressed β-catenin/TCF transcriptional activity. These results indicate that PPARγ negatively regulates epithelial cell turnover via inhibition of β-catenin movement into the nucleus, resulting in the inhibition of β-catenin/TCF–

dependent transcription.

In the present study, we observed that heterodeficiency of PPARγ promoted the formation of ACF, a precancerous pathologic marker in the very early stage of carcinogenesis. These results indicate that PPARγ suppresses tumorigenesis at early stages of initiation. ACF are the formative lesions that lead to adenoma and, consequently, carcinoma. However, PPARγ heterodeficiency did not result in an increased incidence of tumors. These results may indicate that strong activation with non-endogenous ligands is required to suppress tumor progression, although activation of PPARγ by endogenous ligands is sufficient to suppress colonic carcinogenesis at early stages of colon cancer development such as ACF formation (15).

In conclusion, PPARγ regulates colonic epithelial cell turnover via direct interactions with β-catenin, resulting in inhibition of β-catenin translocation into the nucleus. The inhibition of β-catenin translocation prevents β-catenin-mediated transcriptional pathways that are involved in promoting cell proliferation. Our findings indicate that PPARγ plays a role as a physiological regulator of colonic epithelial cell turnover and consequently predisposition to the development of colon cancer.

Acknowledgments

This work was supported in part by a Grant-in-Aid for research on the Third Term Comprehensive Control Research for Cancer from the Ministry of Health, Labor, and Welfare of Japan to AN; a grant from the National Institute of Biomedical Innovation to AN; and a grant from the Ministry of Education, Culture, Sports, Science, and Technology, Japan (KIBAN-B) to AN. RSB was supported by NIH grants DK44319, DK51362, and DK53056.

References

1 Braissant O, Foufelle F, Scotto C, Dauca M, Wahli W. Differential expression of peroxisome proliferator-activated receptors (PPARs): tissue distribution of PPAR-alpha, -beta, and -gamma in the adult rat. Endocrinology. 1996;137:354–366.

2 Lemberger T, Braissant O, Juge-Aubry C, Keller H, Saladin R, Staels B, et al. PPAR tissue distribution and interactions with other hormone-signaling pathways. Ann N Y Acad Sci. 1996; 804:231–251.

3 Tontonoz P, Hu E, Graves RA, Budavari AI, Spiegelman BM. mPPAR gamma 2: tissue-specific regulator of an adipocyte enhancer. Genes Dev. 1994;8:1224–1234.

4 Chawla A, Schwarz EJ, Dimaculangan DD, Lazer MA. Peroxisome proliferator-activated receptor (PPAR) gamma: adipose-predominant expression and induction early in adipocyte differentiation. Endocrinology. 1994;135:798–800.

5 Tontonoz P, Hu E, Spiegelman BM. Stimulation of adipogenesis in fibroblasts by PPAR gamma 2, a lipid-activated transcription factor. Cell. 1994;79:1147–1156.

6 Okuno A, Tamemoto H, Tobe K, Ueki K, Mori Y, Iwamoto K, et al. Troglitazone increases the number of small adipocytes without the change of white adipose tissue mass in obese Zucker rats. J Clin Invest. 1998;101:1354–1361.

7 Cantello BC, Cawthorne MA, Cottam GP, Duff PT, Haigh D, Hindley RM, et al. [[omega-(Heterocyclylamino) alkoxy]benzyl]-2,4-thiazolidinediones as potent antihyperglycemic agents. J Med Chem. 1994;37:3977–3985.

8 Forman BM, Tontonoz P, Chen J, Brun RP, Spiegelman BM, Evans RM. 15-Deoxy-delta 12,14-prostaglandin J_2 is a ligand for the adipocyte determination factor PPAR gamma. Cell. 1995; 83:803–812.

9 Fajas L, Auboeuf D, Raspe E, Schoonjans K, Lefebvre AM, Saladin R, et al. The organization, promoter analysis, and expression of the human PPARgamma gene. J Biol Chem. 1997;272:18779–18789.

10 Suzawa M, Takada I, Yanagisawa J, Ohtake F, Ogawa S, Yamauchi T, et al. Cytokine suppresses adipogenesis and PPAR-gamma function through the TAK1/TAB1/NIK cascade. Nat Cell Biol. 2003;5:224–230.

11 DuBois RN, Gupta R, Brockman J, Reddy BS, Krakow SL, Lazar MA. The nuclear eicosanoid receptor, PPARgamma, is aberrantly expressed in colonic cancers. Carcinogenesis. 1998; 19:49–53.

12 Lefebvre AM, Chen I, Desreumaux P, Najib J, Fruchart JC, Geboes K, et al. Activation of the peroxisome proliferator-activated receptor gamma promotes the development of colon tumors in C57BL/6J-APCMin/+ mice. Nat Med. 1998;4:1053–1057.

13 Saez E, Tontonoz P, Nelson MC, Alvarez JG, Ming UT, Baird SM, et al. Activators of the nuclear receptor PPARgamma enhance colon polyp formation. Nat Med. 1998;4:1058–1061.

14 Sarraf P, Mueller E, Jones D, King FJ, DeAngelo DJ, Partridge JB, et al. Differentiation and reversal of malignant changes in colon cancer through PPARgamma. Nat Med. 1998;4:1046–1052.

15 Osawa E, Nakajima A, Wada K, Ishimine S, Fujisawa N, Kawamori T, et al. Peroxisome proliferator-activated receptor gamma ligands suppress colon carcinogenesis induced by azoxymethane in mice. Gastroenterology. 2003;124:361–367.

16 Tanaka T, Kohno H, Yoshitani S, Takashima S, Okumura A, Murakami A, et al. Ligands for peroxisome proliferator-activated receptors α and γ inhibit chemically induced colitis and formation of aberrant crypt foci in rats. Cancer Res. 2001;61:2424–2428.

17 Niho N, Takahashi M, Shoji Y, Takeuchi Y, Matsubara S, Sugimura T, et al. Dose-dependent suppression of hyperlipidemia and intestinal polyp formation in Min mice by pioglitazone, a PPAR gamma ligand. Cancer Sci. 2003;94:960–964.

18 Niho N, Takahashi M, Kitamura T, Shoji Y, Itoh M, Noda T, et al. Concomitant suppression of hyperlipidemia and intestinal polyp formation in Apc-deficient mice by peroxisome proliferator-activated receptor ligands. Cancer Res. 2003;63:6090–6095.

19 Kiecker C, Niehrs C. Amorphogen gradient of Wnt/beta-catenin

signaling regulates anteroposterior neural patterning in Xenopus. Development. 2001;128:4189–4201.
20 Watson SA. Oncogenic targets of beta-catenin-mediated transcription in molecular pathogenesis of intestinal polyposis. Lancet. 2001;357:572–573.
21 Bienz M, Clevers H. Linking colorectal cancer to Wnt signaling. Cell. 2000;103:311–320.
22 Kwong KY, Zou Y, Day CP, Hung MC. The suppression of colon cancer cell growth in nude mice by targeting beta-catenin/TCF pathway. Oncogene. 2002;21:8340–8346.
23 Wilson AJ, Velcich A, Arango D, Kurland AR, Shenoy SM, Pezo RC, et al. Novel detection and differential utilization of a c-myc transcriptional block in colon cancer chemoprevention. Cancer Res. 2002;62:6006–6010.
24 Tetsu O, McCormick F. Beta-catenin regulates expression of cyclin D1 in colon carcinoma cells. Nature. 1999;398:422–426.
25 Alrawi SJ, Schiff M, Carroll RE, Dayton M, Gibbs JF, Kulavlat M, et al. Aberrant Crypt Foci. Anticancer Res. 2006;26:107–119.
26 Girnun GD, Smith WM, Drori S, Sarraf P, Mueller E, Eng C, et al. APC-dependent suppression of colon carcinogenesis by PPARgamma. Proc Natl Acad Sci U S A. 2002;99:13771–13776.
27 Carbone GM, McGuffie E, Napoli S, Flanagan CE, Dembech C, Negri U, et al. DNA binding and antigene activity of a daunomycin-conjugated triplex-forming oligonucleotide targeting the P2 promoter of the human c-myc gene. Nucleic Acids Res. 2004;32:2396–2410.
28 Jung C, Kim RS, Lee SJ, Wang C, Jeng MH. HOXB13 homeodomain protein suppresses the growth of prostate cancer cells by the negative regulation of T-cell factor 4. Cancer Res. 2004;64:3046–3051.
29 Kubota N, Terauchi Y, Miki H, Tamemoto H, Yamauchi T, Komeda K, et al. PPAR gamma mediates high-fat diet-induced adipocyte hypertrophy and insulin resistance. Mol Cell. 1999;4:597–609.
30 Fearon ER, Vogelstein B. A genetic model for colorectal tumorigenesis. Cell. 1990;61:759–767.
31 Roncucci L, Pedroni M, Vaccina F, Benatti P, Marzona L, De Pol A. Aberrant crypt foci in colorectal carcinogenesis. Cell and crypt dynamics. Cell Proliferations. 2000;33:1–18.
32 Lengauer C, Kinzler KW, Vogelstein B. Genetic instabilities in human cancers. Nature. 1998;396:643–649.
33 Risio M, Coverlizza S, Ferrari A, Cadelaresi GL, Rossini FP. Immunohistochemical study of epithelial cell proliferation in hyperplastic polyps, adenomas, and adenocarcinomas of the large bowel. Gastroenterology. 1988;94:899–906.
34 Deschner EE, Maskens AP. Significance of the labeling index and labeling distribution as kinetic parameters in colorectal mucosa of cancer patients and DMH treated animals. Cancer. 1982;50:1136–1141.
35 Macarthur M, Hold GL, EL-Omar EM. Inflammation and cancer II. Role of chronic inflammation and cytokine gene polymorphisms in the pathogenesis of gastrointestinal malignancy. Am J Physiol Gastrointestinal Liver Physiol. 2004;286:G515–G520.
36 Cesario RM, Stone J, Yen WC, Bissonnette RP, Lamph WW. Differentiation and growth inhibition mediated via the RXR:PPARgamma heterodimer in colon cancer. Cancer Lett. 2006;240:225–233.
37 Nakajima A, Wada K, Miki H, Kubota N, Nakajima N, Terauchi Y, et al. Endogenous PPAR gamma mediates anti-inflammatory activity in murine ischemia-reperfusion injury. Gastroenterology. 2001;120:460–469.
38 Shimada T, Kojima K, Yoshiura K, Hiraishi H, Terano A. Characteristics of the peroxisome proliferator activated receptor gamma (PPARgamma) ligand induced apoptosis in colon cancer cells. Gut. 2002;50:658–664.

Endocrine Journal 2008, **55** (3), 515–522

Molecular Mechanism of Moderate Insulin Resistance in Adiponectin-Knockout Mice

WATARU YANO*, NAOTO KUBOTA*,**,***, SHINSUKE ITOH*, TETSUYA KUBOTA*,***,****, MOTOHARU AWAZAWA*, MASAO MOROI****, KAORU SUGI****, ISEKI TAKAMOTO*,**,***, HITOMI OGATA#, KUMPEI TOKUYAMA#, TETSUO NODA##, YASUO TERAUCHI###, KOHJIRO UEKI* AND TAKASHI KADOWAKI*,**,***

**Department of Diabetes and Metabolic Disease, Graduate School of Medicine, University of Tokyo, Tokyo, Japan*
***Translational Systems Biology and Medicine Initiative, University of Tokyo, Tokyo, Japan*
****Division of Applied Nutrition, National Institute of Health and Nutrition, Tokyo, Japan*
*****Division of Cardiovascular Medicine, Toho University, Ohashi Hospital, Tokyo, Japan*
#Graduate School of Comprehensive Human Sciences, University of Tsukuba, Tsukuba, Japan
##Department of Cell Biology, Japanese Foundation for Cancer Research-Cancer Institute, Tokyo, Japan
###Department of Endocrinology and Metabolism, Yokohama City University Graduate School of Medicine, Yokohama, Japan

Abstract. Adiponectin has been proposed to act as an antidiabetic adipokine, suppressing gluconeogenesis and stimulating fatty acid oxidation in the liver and skeletal muscle. Although adiponectin-knockout (adipo(–/–)) mice are known to exhibit insulin resistance, the degrees of insulin resistance and glucose intolerance are unexpectedly only moderate. In this study, the adipo(–/–) mice showed hepatic, but not muscle, insulin resistance. Insulin-stimulated phosphorylation of IRS-1 and IRS-2 was impaired, the IRS-2 protein level was decreased, and insulin-stimulated phosphorylation of Akt was decreased in the liver of the adipo(–/–) mice. However, the triglyceride content in the liver was not increased in these mice, despite the decrease in the PPARalpha expression involved in lipid combustion, since the expressions of lipogenic genes such as SREBP-1 and SCD-1 were decreased in association with the increased leptin sensitivity. Consistent with this, the down-regulation SREBP-1 and SCD-1 observed in the adipo(–/–) mice was no longer observed, and the hepatic triglyceride content was significantly increased in the adiponectin leptin double-knockout (adipo(–/–)ob/ob) mice. On the other hand, the triglyceride content in the skeletal muscle was significantly decreased in the adipo(–/–) mice, probably due to up-regulated AMPK activity associated with the increased leptin sensitivity. In fact, these phenotypes in the skeletal muscle of these mice were no longer observed in the adipo(–/–)ob/ob mice. In conclusion, adipo(–/–) mice showed impaired insulin signaling in the liver to cause hepatic insulin resistance, however, no increase in the triglyceride content was observed in either the liver or the skeletal muscle, presumably on account of the increased leptin sensitivity.

Key words: Adiponectin, Insulin resistance, Adiponectin-knockout mice, Euglycemic-hyperinsulinemic clamp.
(*Endocrine Journal* **55**: 515–522, 2008)

ADIPONECTIN (also known as Acrp30) [1–4] is a hormone secreted by adipocytes that acts as a major antidiabetic adipokine. Plasma adiponectin levels are decreased in obesity, insulin resistance and type 2 diabetes mellitus [1–4]. Decreased adiponectin has been implicated in the development of insulin resistance in obesity, which has been shown to be reversed by replenishment of adiponectin [5–7]. This insulin-sensitizing effect of adiponectin seems to be mediated by the inhibition of gluconeogenesis in the liver and stimulation of fatty acid oxidation via activation of AMP-activated protein kinase (AMPK) and peroxi-

Received: March 25, 2008
Accepted: March 26, 2008
Correspondence to: Takashi KADOWAKI, M.D., Ph.D. Department of Metabolic Diseases, Graduate School of Medicine, University of Tokyo, 7-3-1 Hongo, Bunkyo-ku, Tokyo 113-8655, Japan.
Abbreviations: EGP, Endogenous Glucose Production; Rd Rate of disappearance

some proliferator-activated receptor (PPAR) alpha in the liver and skeletal muscle [8–12]. Thus, adiponectin ameliorates insulin resistance in both the liver and skeletal muscle.

Adiponectin-knockout (adipo(–/–)) mice have been described mainly by four groups. We reported that adipo(–/–) mice showed insulin resistance [13], indicating that adiponectin acts as an insulin-sensitizing hormone *in vivo*. Maeda *et al.* reported that adipo(–/–) mice fed a normal diet failed to show insulin resistance and glucose intolerance [14]. Ma *et al.* described the absence of insulin resistance and unexpectedly, increased fatty acid oxidation, in the skeletal muscle of adipo(–/–) mice [15]. Nawrocki *et al.* described that adipo(–/–) mice exhibited hepatic, but not muscle, insulin resistance, and increased endogenous glucose production (EGP), with absence of any change in the rate of disappearance (Rd) of glucose during the euglycemic-hyperinsulinemic clamp study [16]. However, the degrees of insulin resistance and glucose intolerance were unexpectedly moderate in these adipo(–/–) mice [13, 15, 16]. We recently reported increased leptin sensitivity in adipo(–/–) mice [17]. Leptin is known to decrease the expressions of lipogenic genes and also the triglyceride content in the liver [18, 19] and, it has also been shown to activate AMPK in the skeletal muscle [20]. In fact, muscle AMPK activity was shown to be increased in the adipo(–/–) mice [17]. In this study, we investigated the molecular mechanisms of the insulin resistance observed in the adipo(–/–) and adiponectin/leptin double-knockout (adipo(–/–)ob/ob) mice.

Materials and methods

Animals

Mice lacking adiponectin were generated as described previously [13, 21]. Adiponectin/leptin double-knockout mice and ob/ob mice were generated by intercrossing of adipo(+/–)ob/+ mice [21]. The mice were allowed free access to water and ordinary laboratory diet. All experiments in this study were conducted on littermate male mice. The animal care and procedures of the experiments were approved by the Animal Care Committee of the University of Tokyo.

Euglycemic-hyperinsulinemic clamp study

A clamp study was carried out as described previously [21]. A catheter was inserted into the jugular vein 2-3 days prior to the clamp study. After overnight food deprivation, insulin was injected constitutively by intravenous infusion at 4 mU/kg/min, and 50% glucose solution enriched to 20% with 6,6-d_2 glucose as tracer was injected to maintain the blood glucose at about 120 mg/dl under conscious and unstressed conditions. Blood was sampled via tail tip bleeds at 90, 105 and 120 min to determine the rate of glucose disappearance (Rd) and endogenous glucose production (EGP).

RNA preparation and analysis

Tissue samples were homogenized to isolate RNA with ISOGEN reagent (Wako, Japan) and analyzed by northern blotting and real-time quantitive PCR. Northern blotting for PPARalpha and SREBP-1 mRNA was carried out as described previously [6, 19]. For real-time quantitive PCR, the ABI 7900 sequence detection system (Applied Biosystems, CA, USA) was used. The RNA sample was processed with TURBO DNase (Ambion, TX, USA) before reverse transcription to synthesize cDNA. 36B4 mRNA was used as the internal control. The primer sets for PEPCK and G6Pase were purchased from Applied Biosystems. The sequences of the primer sets for SREBP-1c, PPARalpha and 36B4 were as follows [22]; SREBP-1c: forward primer, ATCGGCGCGGAAGCTGTCGGGGTAG CGTC; reverse primer, TGAGCTGGAGCATGTCT TCAA; probe, FAM-ACCACGGAGCCATGGATT GCACATT-TAMRA. PPARalpha: forward primer, CAACGGCGTCGAAGACAAA; reverse primer, GACGGTCTCCACGGACATG; probe, FAM-CAGAGGTCCGATTCTTCCACTGCTGC-TAMRA. 36B4: forward primer, TGCCACACTCCATCAT CAATG; reverse primer, CCGCAAATGCAGATG GATC; probe, FAM-CCCACTTACTGAAAAGGT CAAGGCCTTCCTG-TAMRA.

Measurement of the tissue triglyceride content

Tissue homogenate was extracted with 2:1 (vol/vol) chloroform/methanol, and the triglyceride content was determined as described previously [22]. In brief, chloroform/methanol was added to the homogenate and shaken for 15 min. After centrifugation at 14,000

rpm for 10 min, the organic layer was collected. This extraction step was repeated three times. The collected sample was dried and resuspended in 1% Triton X-100/ ethanol, and measured using L-type Wako (Wako, Japan).

Immunoprecipitation and western blotting

Immunoprecipitation and western blot analyses were carried out as described previously [23]. Tissue lysate was immunoprecipitated with anti-IRS-1 antibody or anti-IRS-2 antibody (Upstate, VA, USA) and blotted with an anti-phospho-tyrosine (anti-pY) antibody (Upstate, VA, USA) to assess the degree of phosphorylation of IRS-1 or IRS-2. For the western blot analyses, antibodies against Akt, phospho-Akt, AMPK and phospho-AMPK (Cell Signaling Technology, MA, USA) were used.

Statistics

All values were expressed as means ± SEM. The statistical significances of differences were calculated using the *t*-test.

Results

The euglycemic-hyperinsulinemic clamp study revealed hepatic insulin resistance in the adipo(–/–) mice

We carried out the euglycemic-hyperinsulinemic clamp study using the tracer technique in the wild-type and adipo(–/–) mice. Significant decrease of the GIR was observed in the adipo(–/–) mice as compared with that in the wild-type mice (Fig. 1A), indicating that the adipo(–/–) mice indeed exhibited insulin resistance, as previously reported [13]. Adipo(–/–) mice showed similar Rd to the wild-type mice, but significantly increased EGP. (Fig. 1B, C). The expressions of PEPCK (Fig. 1D) and G6Pase (Fig. 1E), which are involved in gluconeogenesis, were up-regulated during the euglycemic-hyperinsulinemic clamp study in the adipo(–/–) mice, indicating the hepatic insulin resistance in the adipo(–/–) mice.

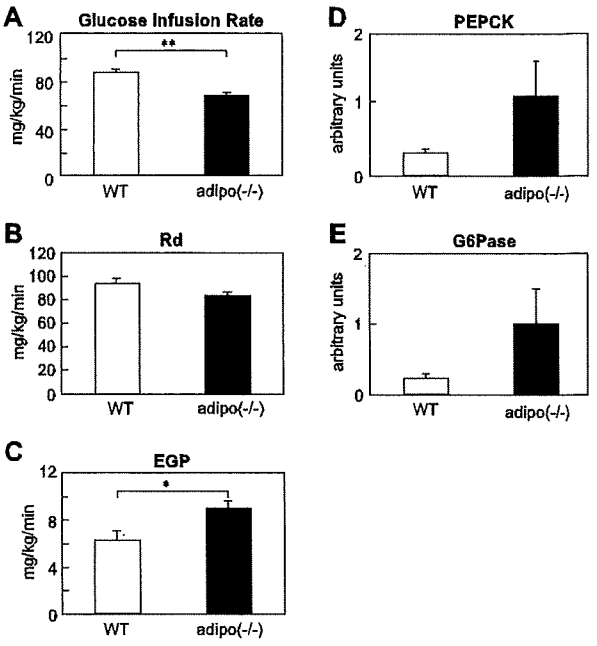

Fig. 1. The euglycemic-hyperinsulinemic clamp study revealed hepatic insulin resistance in the adipo(–/–) mice. (A-E) Glucose infusion rate (GIR) (A), rate of glucose disappearance (Rd) (B), endogenous glucose production (EGP) (C), PEPCK (D) and G6Pase (E) mRNA levels in the liver during the euglycemic-hyperinsulinemic clamp study. All values are expressed as means ± SEM of data (n = 7) obtained from the analysis of wild-type (*open bars*) and adipo(–/–) mice (*closed bars*). *$p<0.05$, **$p<0.01$.

Impaired insulin signaling in the liver of the adipo(–/–) mice

Insulin signaling was investigated in the liver and the skeletal muscle of the adipo(–/–) mice. Insulin-stimulated tyrosine phosphorylation of IRS-1 was significantly decreased and that of IRS-2 was markedly decreased in the liver of the adipo(–/–) mice as compared with that in the liver of the wild-type mice (Fig. 2A). The protein level of IRS-2 was significantly decreased, while that of IRS-1 was not altered (Fig. 2A). Insulin-stimulated phosphorylation of Akt was also significantly reduced in the adipo(–/–) mice (Fig. 2B). In the skeletal muscle, the insulin-stimulated tyrosine phosphorylation level of IRS-1 was similar in the wild-type and adipo(–/–) mice (Fig. 2C). The insulin-stimulated phosphorylation level of Akt was also similar in the two genotypes (Fig. 2D). These data indicate impairment of hepatic insulin signaling in the adipo(–/–) mice.

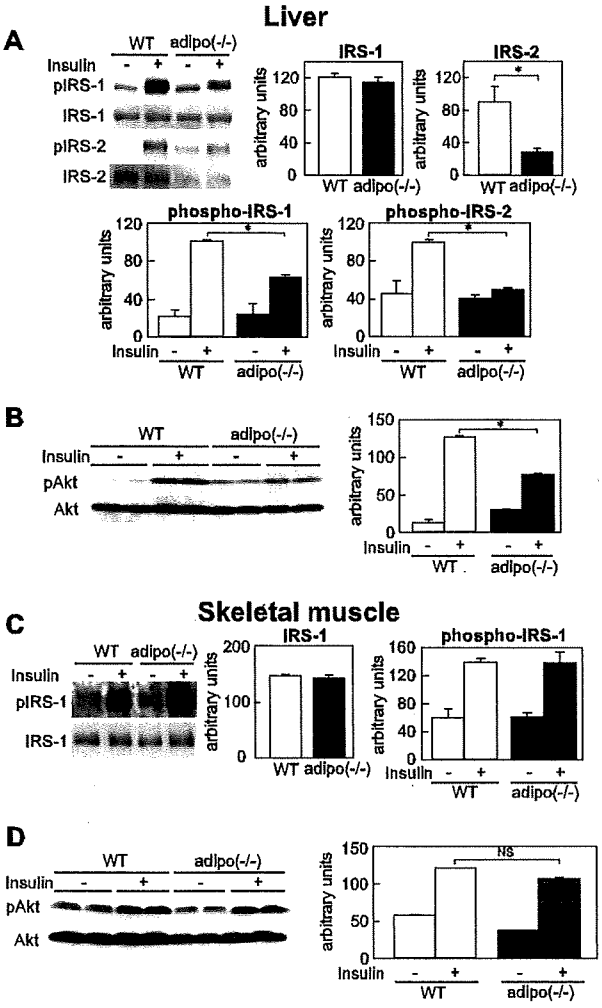

Fig. 2. Impaired insulin signaling in the liver of the adipo(–/–) mice.
(A) Insulin-stimulated tyrosine phosphorylation of IRS-1 and IRS-2 in the liver. Quantification of the protein levels (*upper, right*) and phosphorylation levels of IRS-1 and IRS-2 (*lower*). (B) Insulin-stimulated phosphorylation of Akt in the liver. (C) Insulin-stimulated tyrosine phosphorylation of IRS-1 in the skeletal muscle. Quantification of the protein level (*middle*) and phosphorylation level of IRS-1 (*right*). (D) Insulin-stimulated phosphorylation of Akt in the skeletal muscle. All values are expressed as means ± SEM of data (n = 4) obtained from the analysis of wild-type (*open bars*) and adipo(–/–) mice (*closed bars*). *$p<0.05$.

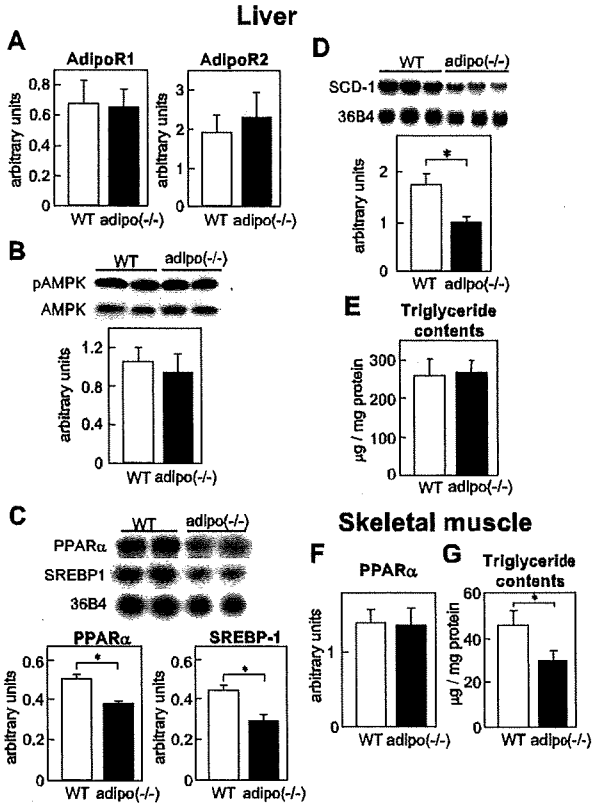

Fig. 3. Hepatic triglyceride content was not elevated and the expressions of lipogenic genes were down-regulated in the adipo(–/–) mice.
(A) AdipoR1 and AdipoR2 mRNA expression levels in the liver (n = 3). (B) AMPK phosphorylation in the liver (n = 8–10). (C-D) The mRNA levels of PPARalpha, SREBP-1 (C) and SCD-1 (D) in the liver (n = 4–5). (E) Hepatic triglyceride content (n = 11–14). (F) PPARalpha expression level in the skeletal muscle (n = 5). Triglyceride content (G) in the skeletal muscle (n = 5). All values are expressed as means ± SEM of data obtained from the analysis of wild-type (*open bars*) and adipo(–/–) mice (*closed bars*). *$p<0.05$.

Hepatic triglyceride content was not elevated and the expressions of lipogenic genes were down-regulated in the adipo(–/–) mice

We next investigated the lipid metabolism in the liver of these mice. No significant differences in the expression levels of the adiponectin receptors AdipoR1 and AdipoR2 [24] were observed between the wild-type and adipo(–/–) mice (Fig. 3A). While the degree of AMPK phosphorylation remained unchanged (Fig. 3B), significant down-regulation of PPARalpha